JOURNAL OF MATERIALS SCIENCE 35 (2000) 967–973

Dissolution mechanisms of boro-silicate glass fibres in saline solution with added dissolved silica

P. BAILLIF*, B. CHOUIKHI, J. C. TOURAY
Université d'Orléans— UMR n° 6530, ESEM, 8, Rue Léonard de Vinci, 45072 Orléans Cedex 2, France
E-mail: Patrick.Baillif@univ-orleans.fr

Experiments of dissolution of a soluble boro-silica glass were performed at 37 °C in a saline solution without and with 50, 75 and 100 ppm of added silica. After reaction silica concentration was measured by AAS and colorimetry and fibers were investigated by SEM-EDS and XPS. The results give informations on the dissolution velocity of the glass and the factors controlling the formation rate of the gel layer and its composition. The dissolution velocity measured at the unaltered glass-gel interface is not significantly decreased by the silica concentration in solution whatever its origin (leaching of the glass fibres or initial addition). Accordingly, gel formation is controlled by the chemical reactions rate at, or near, the boundary of the unaltered core. The composition and the stucture of the gel layer are depending on the silica concentration in solution above a threshold of about 50 ppm. The framework of the gel appears to play the more important role in the dissolution velocity of the glass.

1. Introduction

The knowledge of long-term dissolution rates of artificial glasses in geological environments has important practical applications (e.g.: nuclear wastes disposal). In this respect [1, 2], a two-step approach may be developed involving i) an experimental identification of the short-term aqueous corrosion mechanisms and ii) a long term extrapolation using a geochemical modelling based on the precipitation of silicate phases. Accordingly, the phenomenology of glass-water interactions has to be precisely known.

Since the pioneering works of Douglas and Izard [3], Douglas and El Shamy [4] Boksay et al. [5] the dissolution of both natural and artificial silicate glasses has been studied by different authors [6–10]. Three important classes of leaching reactions have been recognized and discussed by Casey and Bunker [11]: (i) hydration, (ii) ion exchange reactions, leading to the formation of a leached material by replacement of modifier cations with hydrogen ions and (iii) hydrolysis reactions.

The dissolution kinetics of the gel layer is dependent on the composition of the solution and, for example, the general equation by Aagaard and Helgeson [12] has been applied to borosilicate glass alteration [13]. In the simplest rate equation [13] the hydrolysis of the Si–O bond is supposed to be the limiting step in the dissolution process. Far from "saturation", the dissolution rate (first order law) is a simple function of the activity of H_4SiO_4. Close to "saturation", the corrosion rate of a borosilicate glass drops by several orders of magnitude from the initial rate but a steady state is never reached. The reasons for such a continuous release of SiO_2 remain obscure and different explanations have been suggested [8, 14].

The gel layer may be considered as a modified residual glass "skeleton", the material leached after ionic exchange beeing repolymerized into a porous silica-rich network [10]. A synthesis of all the observations made on gel layers formed after corrosion of the borosilicate reference glass R7T7 used for the storage of nuclear wastes [8] is in agreement with this conclusion.

In contact with water, glass is superficially hydrated. Then, through ionic exchange is created a leached surface whose evolution gives birth after hydrolysis then liberation of dissolved silica and local repolymerization to a porous gel layer.

Indeed, an issue generally not adressed is the distinction of hydrolysis reactions resulting in gel formation with liberation of mobile silica from other developing at the gel-solution limit (gel dissolution). Both may lead to an increase of dissolved silica but a priori they are not controlled by the same factors.

To adress this issue requires a method for determining the thickening rate of the gel layer under unsteady state conditions. In this respect, experiments using glass fibres and SEM-EDS studies of their sections after corrosion, permit a geometrical determination of the thickening rate of the gel, as well as its chemical characterization [15, 16].

* Author to whom all correspondence should be addressed.

2. Materials and method

2.1. Solid materials

A relatively soluble boro-silicate glass (courtesy: Saint-Gobain Recherche, Aubervilliers, France) was selected for this study. Indeed, the composition of the glass fibres was as following: 61% SiO_2, 16% Na_2O, 11% B_2O_3, 7% CaO, 3% MgO, 1% Al_2O_3 and 1% P_2O_5. Fibres of textile type with uniform diameters (10 ± 1 μm) were used.

2.2. Reacting solutions

The dissolution of the fibres was investigated in a saline solution (K0) previously used by Scholze and Potter [17, 18] which contained as main components NaCl, $NaHCO_3$, NH_4Cl and glycine. The pH of the solution was 7.6 ± 0.2. Soluble silica, introduced as $SiCl_4$, was added to K0 solution at amounts of 50, 75 and 100 ppm (K50, K75 and K100 solution respectively).

2.3. Experimental procedures

For each run 30 mg of fibres (about 3 cm long) were introduced, on a Teflon grid, in a Teflon reactor with 250 ml of solution ($S/V = 0.192$ cm^{-1}). The reactor was then introduced in an oven regulated at 37 ± 1°C for leaching durations from 1 day to 60 days. Experiments were carried out in non stirred solutions. After each run, the fibres were pulled out, rinsed with deionized water, and dried for weighing and investigations by XPS and SEM. The solution was filtered with a 0.45 μm pore size filter before determination of the silica concentration by AAS (HITACHI Z-8100) and by a colorimetric method (yellow silico-molybdate complex). Al was looked for but not detected by AAS (Al $<$ 10 ppb).

2.4. Investigations of reacted fibres

The surface of the fibres was directly analysed by XPS using an AEI ES200B spectrometer fitted with a Mg anode. Water content was measured by micro-GTA using a CAHN RG electrobalance. SEM studies and EDS analysis were performed with a JEOL WINSEM apparatus on polished sections of fibres included in epoxy resin.

3. Results and interpretations

3.1. Relative weight loss

The relative weight loss was calculated as follows.

$$p = \frac{m_0 - m_t}{m_0} \tag{1}$$

where m_0 is the initial mass of the glass fibres (in g) and m_t the mass of glass fibres at time t (in g).

The dissolution kinetics of the glass fibres, expressed by relative weight loss (p), are displayed in Fig. 1. We notice that a plateau is reached for the same duration, at about 18–20 days, whatever the concentration of the initial added silica ($[SiO_2]_i$). On the other hand, we notice a decreasing of the plateau value (p_f) in relation with the amount of added silica.

TABLE I Correlation between the plateau values of the relative weigth loss (p_f) and the silica concentration ($[SiO_2]_f$) in ppm when the glass dissolution is complete in the four different solutions

	K0	K50	K75	K100
p_f	.90	.87	.76	.63
$[SiO_2]_f$	66	63	55	52

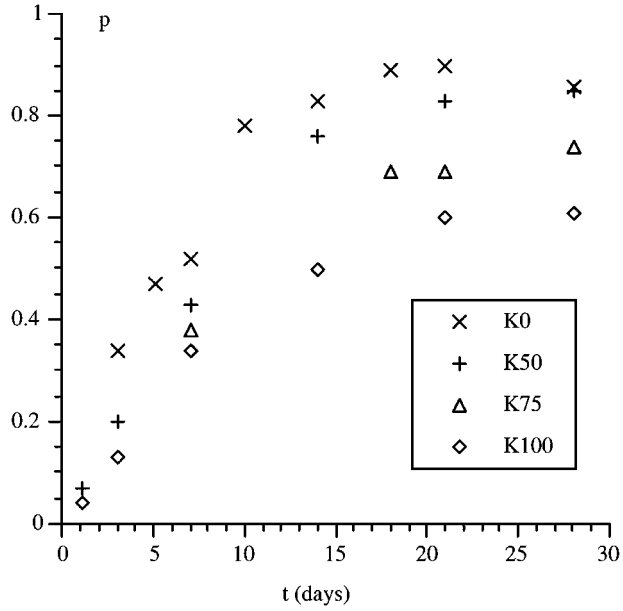

Figure 1 Variation of the relative weight loss (p) versus time (in days).

3.2. Solution analysis

The pH of the solution slightly increases at 8.3 ± 0.3 during the dissolution. Analysis of silica in solution performed by AAS or a colorimetric method give identical results. This confirms that silica in solution is only as H_4SiO_4 form. To compare the differents solutions the value of $[SiO_2]_i$ was deduced of the measured concentration of soluble silica.

The kinetics of dissolution as soluble silica are shown in Fig. 2. As observed for the weight loss, no significant concentration variation occurs after about 20 days. Moreover, weight loss and soluble silica concentration are well correlated. This relation is shown in Table I for the plateau values.

3.3. Scanning electron microscopy

SEM observations of cross sections of altered fibers (Fig. 3) show a thicker gel layer when silica was added in solution. Moreover, for experiments with $[SiO_2]_i = 100$ ppm, the bulk radius of the reacted fibres remains nearly constant while it decreases with leaching time for other runs. Then, when the glass is entirely dissolved ($t = t_f$, about 20 days) the diameter of the residual gel is about 4 μm without added silica and 9 μm with 100 ppm of added silica. A schematic representation of the dissolution kinetic of the fibres is displayed in Fig. 4 for K0 and K100 experiments.

TABLE II Comparaison between the Al/Si atomic ratio, determined at the surface of the hydrated layer by XPS, and measured in the whole layer by EDS. Na/Si ratio was only determined from XPS analyses

	Time (day)	Al/Si (XPS)	Al/Si (EDS)	Na/Si (XPS)
K0	3	0.15	—	0.24
	7	0.18	—	0.21
	10	0.23	0.14	0.15
	14	0.17	0.17	0.19
	18	0.24	0.17	0.14
	21	0.19	0.17	0.13
	28	0.24	0.15	0.19
	60	0.24	0.17	0.17
K50	3	0.15	—	0.14
	7	0.14	—	0.10
	14	0.16	0.12	0.10
	21	0.18	0.11	0.15
	28	0.17	0.10	0.10
K75	18	0.09	—	0.04
	21	0.09	0.07	0.02
	28	0.12	—	0.06
K100	3	0.06	—	0,07
	7	0.10	0.05	0.06
	14	0.07	0.03	0.06
	21	0.08	0.04	0.07
	28	0.06	0.04	0.04
	60	0.09	0.04	0.05

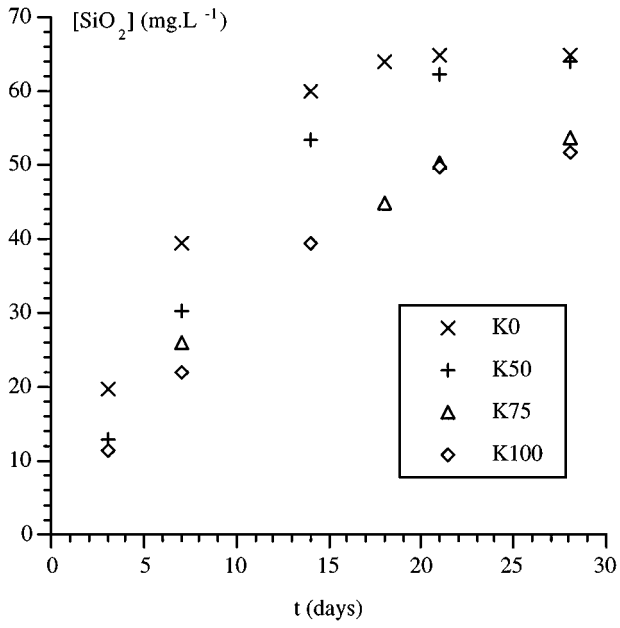

Figure 2 Variation of the concentration of SiO_2 (in $mg \cdot L^{-1}$) versus time (in days). For K50, K75 and K100 experiments the initial value (50, 75 or 100 $mg \cdot L^{-1}$) was substracted from measured concentration.

3.4. Composition of the hydrated superficial layer

XPS and EDS analysis data (Table II) indicate that the hydrated layer is essentially siliceous with variable amounts of aluminium and sodium. The Si/Al atomic ratio of the outer part of the hydrated layer, determined by XPS on a 6 nm scale depth, is depending on $[SiO_2]_i$ but does not vary significantly during each run. The Si/Al ratio determined, for largely reacted fibres, by EDS, which gives a mean composition on one to two micrometers, is lower than the former.

Thermogravimetric analysis of totally reacted fibres (i.e. without unreacted glass core) complements the characterization of the hydrated product. The Table III gives, for K0, K50, K75 and K100 experiments and per 1 mole of Al_2O_3, the molar composition of the hydrated surface layers calculated from XPS (outer values of Al_2O_3, SiO_2 and Na_2O), EDS (mean values of Al_2O_3 and SiO_2) and thermogravimetric data (mean values of H_2O).

TABLE III Outer and mean molar composition of the hydrated surface layer

	K0		K50		K75		K100	
	Outer	Mean	Outer	Mean	Outer	Mean	Outer	Mean
Al_2O_3	1	1	1	1	1	1	1	1
SiO_2	10	12	12	18	20	28	26	52
Na_2O	1	—	1	—	1	—	1	—
H_2O	—	18	—	20	—	32	—	55

The agreement between outer and mean Si/Al ratio is good for experiments without added silica, as previouly described [15], but poorer and poorer as the initial added silica concentration increases.

3.5. Dissolution velocity

The dissolution velocity of the glass at the unaltered core-hydrated layer interface, v_1 in μm/day, is defined by the relation:

$$v_1 = -r_0 \frac{dz_1}{dt} \tag{2}$$

where $z_1 = r_1/r_0$ is a dimensionless parameter, r_1 the radius of the unaltered core and r_0 the mean radius of the initial glass fibres (i.e. 5 ± 0.5 μm).

Usually, the dissolution kinetics of glasses is characterized by "leaching rates" expressed in $g \cdot cm^{-2} \cdot day^{-1}$ or $mol \cdot cm^{-2} \cdot s^{-1}$ [8], by reference to the solubilization of a glass component (e.g.: B, Na or SiO_2). Indeed, leaching rates are equivalent to dissolution velocities only when glass dissolution is congruent [19] but not when a residual surface layer, which possibly contains this element, is formed, as in the present case. On the other hand, the dissolution velocity can be geometrically measured from cross section of fibres at different durations of reaction and calculated from relative weight loss using a previously described modelling [15].

3.5.1. SEM data

The Fig. 5 shows the variation versus time of z_1 directly determined from SEM photos of cross-sections of the fibres. In this representation, a straight line would reflect a constant dissolution velocity. Actually, the curves present a slight curvature indicating a slowing down with time. The initial dissolution velocity (v_i) determined from the tangent to the experimental curves at $t = 0$, scatters in the range 0.25 to 0.35 μm/day (i.e. 0.30 ± 0.05 μm/day), as indicated in the Fig. 4 by the dashed and the dotted lines respectively, whatever the initial concentration of added silica in solution.

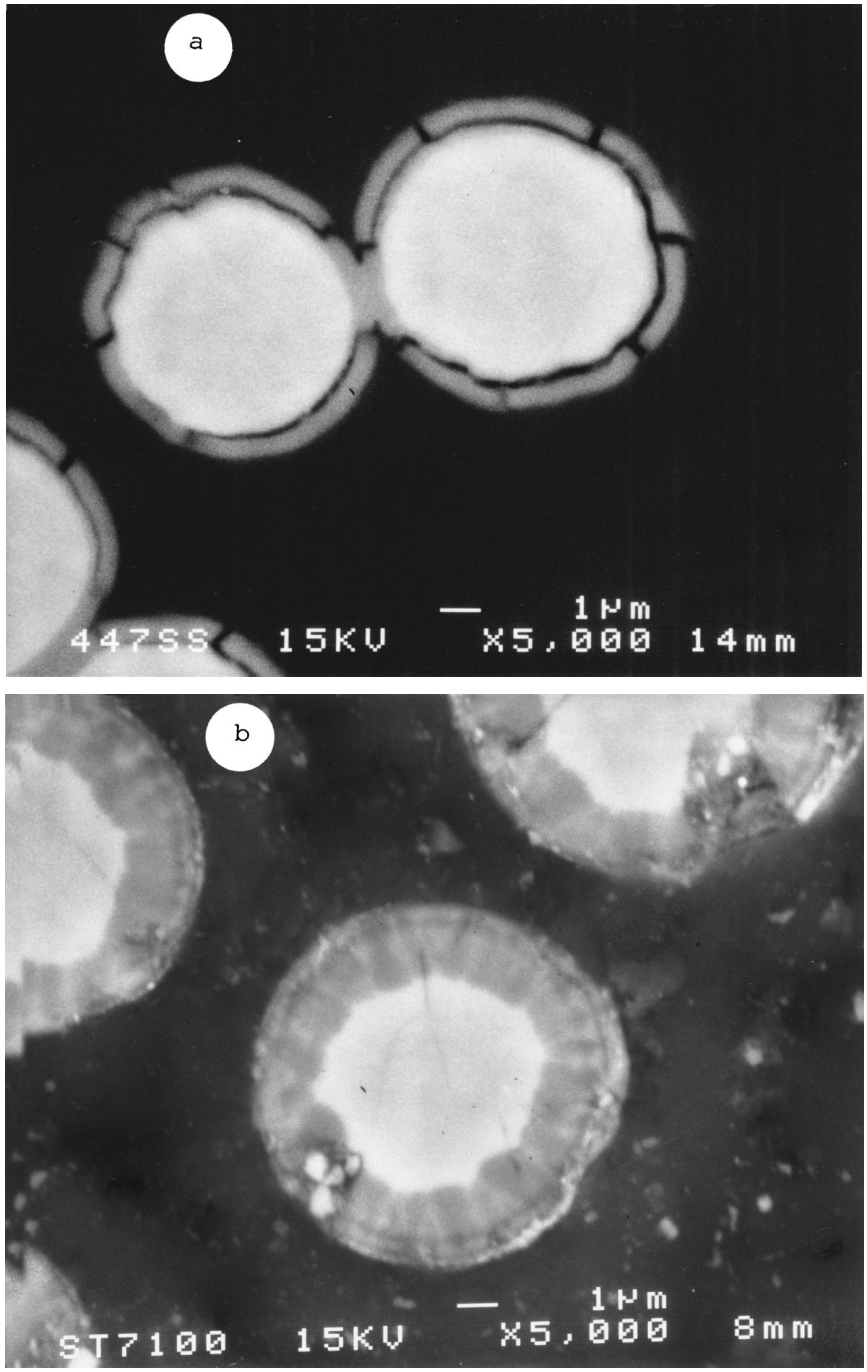

Figure 3 SEM backscattered electron images of the glass fibers (sections) showing the outer gel layer and the unaltered core: a) K50, 7 days; b) K100, 7 days.

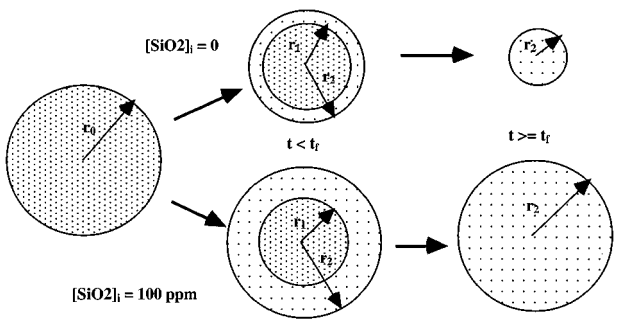

Figure 4 Schematic representation of the dissolution kinetic of the glass fibres without and with 100 ppm of added dissolved silica (K0 and K100 experiments). r_0: initial radius of the fibre; r_1: radius of the unaltered core; r_2: radius of the bulk fibre (with the outer gel layer); t_f: time when the dissolution of the glass fibre is complete (about 20 days).

3.5.2. Modelling

In a previous paper [15] describing the dissolution of the same glass fibres in solutions K0 ($[SiO_2]_i = 0$) was developped a model relating z_1, the relative radius of the unaltered core, to the relative weight loss. Assuming a cylindric shape of the fibres all along their dissolution, one has the relation:

$$z_1 = \frac{r_1}{r_0} = [1 - \beta p]^{1/2} \qquad (3)$$

where β is a dimensionless parameter whose value may be experimentally determined when the dissolution of the glass core is complete.

We note from Equation 3 that if $z_1 = 0$ then $p = p_f$ and $\beta = 1/p_f$.

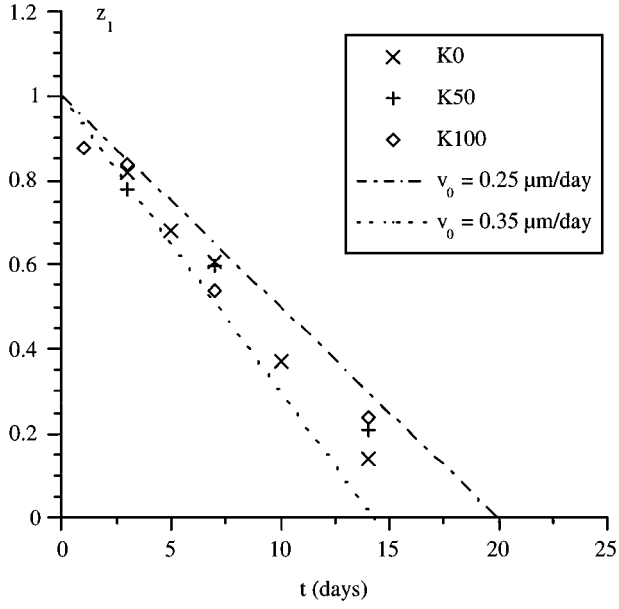

Figure 5 Variation of the relative radius of the unaltered fibre (z_1) measured by SEM versus time (in days). The dotted line corresponds to a dissolution velocity of 0.35 μm · day^{-1} and the dashed line to a dissolution velocity of 0.25 μm · day^{-1}.

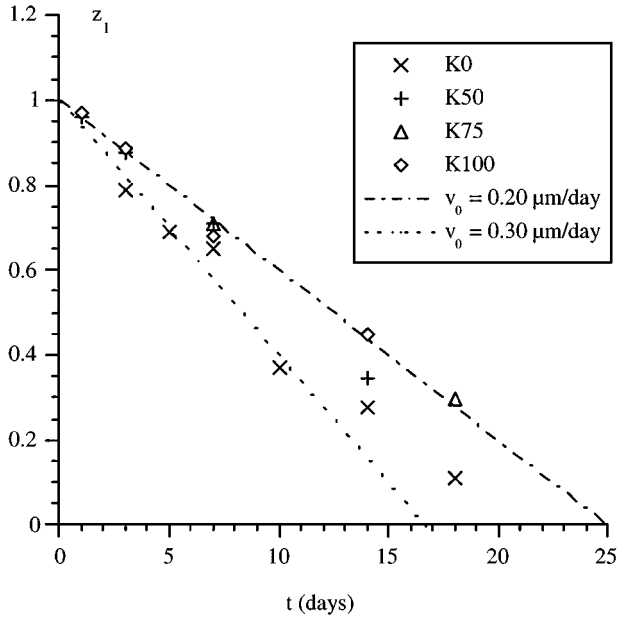

Figure 6 Variation of the relative radius of the unaltered fibre (z_1) calculated from Equation 3, with $p_f = 0.9$, 0.87, 0.76 and 0.63 for respectively K0, K50, K75 and K100 experiments, versus time (in days). The dotted line corresponds to a dissolution velocity of 0.30 μm · day^{-1} and the dashed line to a dissolution velocity of 0.20 μm · day^{-1}.

This model assumes a constant composition of the gel layer all along the dissolution, it is virtually true for $[SiO_2]_i = 0$ but not for other experiments with added silica. However, it is possible for all runs to draw kinetic dissolution curves, as $z_1 = f(t)$ (Fig. 6), using the Equation 3 from the measured relative weight loss and its plateau value (p_f) for β.

The initial dissolution velocities (v_0) estimated from the tangent to the experimental curves at $t = 0$ scatter in the range 0.2 to 0.3 μm/day (i.e. 0.25 ± 0.05 μm/day) as indicated in Fig. 6 by the dashed and the dotted lines respectively.

TABLE IV Mean gel density of fully reacted fibres (ρ_h) determined from the relative weight loss (p_f) and the relative radius of the "fibres" (z_h) observed by SEM when glass dissolution is complete

	K0	K50	K75	K100
p_f	.90	.87	.76	.63
z_h	.36	.44	.70	.92
ρ_h	1.9	1.7	1.2	1.1

Eventually, the estimations of dissolution velocities derived both from SEM data and weight losses give close results. They indicate that dissolution velocity is only slightly modified by addition of silica in solution and that a minor decrease (at least for K0 experiments) is observed when the thickness of the layer is the highest.

3.6. Apparent density of the gel

The mean apparent density of the gel of completely reacted fibres ($z_1 = 0$) may be estimated from SEM photos and the corresponding weigth loss using the following mass-balance equation:

$$\rho_h = \rho \frac{1 - p_f}{z_h^2} \tag{4}$$

with $z_h = e/r_0$ (when $z_1 = 0$ then $z_2 = z_h$), where ρ ($= 2.5$ g/cm^3) is the unaltered glass density, ρ_h the mean density of the hydrated layer in g/cm^3 and e the thickness of the hydrated layer in μm.

The mean density of the gel, calculated with Equation 4, is indicated in the Table IV for the four series of experiments. The results show a decrease of the density, certainly to correlate to an increase of the layer porosity, when the silica concentration in solution is the highest.

3.7. Variation of the gel composition

In a previously described model for $[SiO_2]_i = 0$ [15] the mass of the hydrated layer m_h was correlated to the mass of unreacted glass m_1 by:

$$m_h = \alpha(m_0 - m_1) \tag{5}$$

where α is a dimensionless parameter which represents the mass of the hydrated layer (in g) per g of dissolved glass.

The model assumed that Al was entirely accumulated in the gel layer and that the composition of the layer remained constant during dissolution. The first hypothesis is always confirmed at the sensitivity level used (10 ppb) but the second is virtually correct only if $[SiO_2]_i = 0$. However, for other experiments the variation of the gel composition with $[SiO_2]_i$ is continuous and moderate (except for K100).

The α parameter can be calculated from the alumina concentration of the anhydrous glass ($C_a = 1\%$) and the molecular weigth of the gel per 1 mole of Al_2O_3 (M_h).

$$\alpha = C_a \frac{M_h}{M_a} \tag{6}$$

where M_a is the molecular weight of alumina (=102 g).

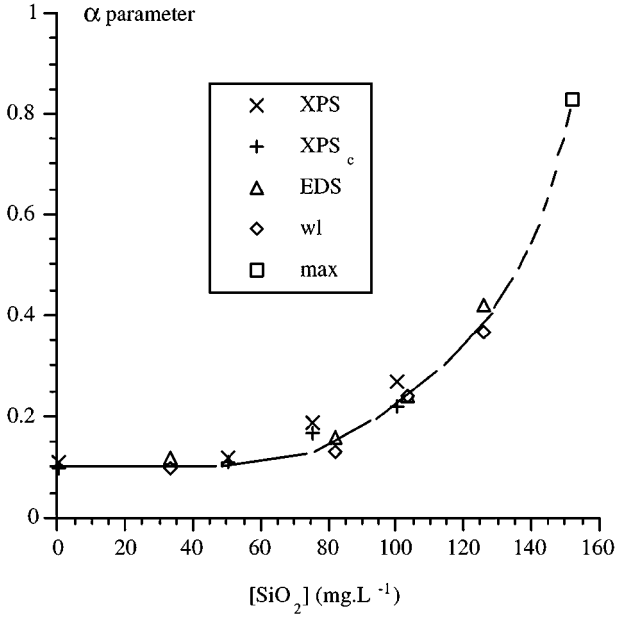

Figure 7 Variation of the α parameter versus silica concentration (in $mg \cdot L^{-1}$). XPS and XPSc: initial values from XPS data with two estimations of the water content, EDS and wl: mean values from EDS data and weight loss, max: calculated maximum value.

Using Equation 6, three estimations of this parameter were calculated: two initial values from the composition of the gel determined by XPS at the beginning of the reaction with two H_2O contents (the mean H_2O content of Table III and the same one corrected by the outer/mean SiO_2 ratio) and one mean value from the mean composition of the gel determined by EDS.

In addition, from the model, another estimation of α parameter (mean value) can be deduced from the plateau value of the weight loss on fully reacted fibres.

$$\alpha = 1 - \frac{1}{\beta} = 1 - p_f \qquad (7)$$

The variation of the α parameter is represented in Fig. 7 versus $[SiO_2]$ for K0, K50, K75 and K100 experiments. The two initial values are plotted at the initial silica concentration and the two mean values at the mean concentration of silica in solution (initial + final concentration divided by 2).

The curve obtained with these different estimations shows that the increase of the α parameter occurs only above a threshold of around 50 ppm of silica. Then, above about 100 ppm of dissolved silica the increase is still higher. Moreover, the maximum value of the α parameter can be calculated from the composition of the glass (with the Si/Al ratio of the glass) and an estimation of the H_2O content. We find a value ($\alpha = 0.82$) compatible with the curve determined from Equations 6 and 7.

4. Discussion and conclusions

Previous experiments, performed in saline solution, have shown that the dissolution velocity of the glass did not appreciably decreased neither with the silica concentration in solution nor with the thickness of the gel layer. New experiments with added silica in the solution corroborate these results even though both composition and thickness of the gel layer are modified. In this respect, the variation of the gel composition is well described by the α parameter which represent the retention factor of peculiar glass components in the gel, mainly Si and Al.

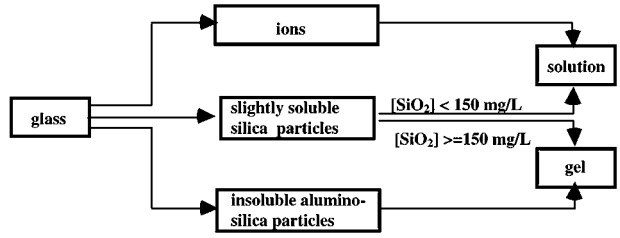

Figure 8 Schematic representation of the glass dissolution with formation of a gel by aggregation of alumino-silica (and silica) particles issued from the breakdown of the glass network.

4.1. Mechanisms of the glass dissolution

A possible explanation of our results is as follows.

The first step of the glass dissolution is the hydration of the solid and consequently the hydrolysis of the more easily hydrolysable bonds ≡Si–O–Na, ≡Si–O–B= and ≡Si–O–Ca– bonds which liberates, on one hand, soluble ions and, on the other hand, slightly soluble silica particles and insoluble alumino-silica particles (Fig. 8). The presence of silica particles is assumed as resulting from lower hydrolysis rate for ≡Si–O–Si≡ bonds. Actually, alumino-silica particles are slightly soluble in renewed solutions as previously demonstrated [15]. In this hypothesis, these reactions lead to the breakdown of the glass network but not to a complete solubilization of the material.

The second step is the hydration of the polymeric silica particles (depolymerization) which liberates soluble monomeric silica according to the following reaction:

$$(SiO_2)_x + 2H_2O \rightarrow (SiO_2)_{x-1} + H_4SiO_4 \qquad (8)$$

The third step is the migration of soluble ions and monomeric silica towards the solution (through the porosity of the gel layer when formed).

The rate of glass dissolution is depending of the nature of the solution. Indeed, it is well known that NaCl acts as a catalyst in the solubilization of silica [20]. However, the first step (breakdown of the glass network) is not significantly slowered by the accumulation of silica in solution as shown by the weak variation of the dissolution velocity during the reaction. On the contrary, the second step (hydration of the polymeric silica particles) and the third step (diffusion of monomeric silica) are depending on the concentration of monomeric silica in solution. If this concentration is low, the silica particles will be completely dissolved and monomeric silica will diffuse towards the solution. When the amount of soluble silica in solution is increased, the hydrolysis of silica particles is slowered and these ones are possibly trapped into the gel layer. In the same way, the gradient of the concentration of

monomeric silica in the gel layer is less important and the diffusion of silica towards the solution is slowered.

Finally, when the solubility (of amorphous silica ?) is reached (at about 150 ppm), the flux of monomeric silica towards the solution is stopped (Fig. 8) and polymeric silica particles no longer dissolve. In other words, steps 2 and 3 no longer occur while the reaction of hydrolysis (step 1) is not stopped as demonstrated by experiments with 100 ppm of added silica (which final concentrations are of about 150 ppm).

4.2. Gel formation

As the breakdown of the glass network leads to the liberation of particles, the gel is assumed to grow, nearby the hydrated glass, by aggregation of non soluble alumino-silica particles and, if the amount of monomeric silica in solution is sufficiently high (i. e. when the reaction (8) is limited), silica particles (Fig. 8). This interpretation is compatible with an increase of the α parameter, above a threshold, with the silica concentration (Fig. 6). In this hypothesis, the threshold value (about 50 ppm as SiO_2) will represent the maximum concentration corresponding to relation 8 with the same rate for dissolution and condensation process.

The gel layer does not modify, in a significant extent, the dissolution rate of the glass (Figs 5 and 6). In other word, the accessibility of water molecules (and OH^- ion) to the glass-gel interface and, consequently, the hydrolysis rate of the easily hydrolysable chemical bonds are not significantly reduced. The porosity of the gel plays an important role in the dissolution process since it facilitates, the hydration of the glass at the glass-gel interface and, at the same time, the migration of the dissolved species towards the solution. In this respect, the thickness and the apparent porosity of the gel layer (Table IV) both increase with the silica concentration in solution.

By another way, the gel composition is fixed during its formation, as indicated by XPS analysis at the gel-solution interface (Table II). Moreover, when the silica concentration is low, the gel framework is deformable as shown by the backward movement of the bulk fibres (Fig. 4 and Table IV). A possible explanation is that the silico-alumina (and silica) particles, which form the gel, are bridged by weak bonds. In this respect, the sodium ion, present in the solution and in the glass, possibly acts as a bridging ion [20]. On the contrary, if the external silica concentration is high, the transformation glass-gel practically occurs without volumetric modification. This result is then compatible with the gel formation by aggregation, near the glass surface, of alumino-silica particles with larger and larger silica particles as silica concentration increases in the solution.

4.3. Rate of dissolution

In a first time, for a given solution, the rate of dissolution (initial velocity) is related to the proportion of easily hydrolysable chemical bonds, i. e., to the glass composition. Then, after the formation of a superficial gel layer, the dissolution rate is essentially depending on the accessibility of water molecules to the surface of the unaltered glass through the gel layer, i. e., to the gel "structure". Two conditions, elevated proportion of easily hydrolysable chemical bonds and, high porosity of the gel layer must be combined to obtain a relatively soluble glass. In this respect, additions of monomeric silica in the initial solution modify the gel structure (and its composition) by increasing its porosity. On the contrary, to have a slightly soluble glass a dense protective gel must be formed during alteration to limit the rate of hydrolysis of $\equiv$Si–O–Si$\equiv$ bonds.

References

1. T. ADVOCAT, Thesis, Univ. Louis Pasteur, Strasbourg, 1991.
2. I. TOVENA, Thesis, Univ. Montpellier II, Montpellier, 1995.
3. R. W. DOUGLAS and J. O. IZARD, *J. Soc. Glass Tech.* **33** (1949) 289.
4. R. W. DOUGLAS and T. M. EL SHAMY, *J. Am. Ceram. Soc.* **30** (1967) 1.
5. Z. BOKSAY, G. BOUQUET and S. DOBOS, *Phys. Chem. Glasses* **9** (1968) 69.
6. J. L. CROVISIER, J. H. THOMASSIN, T. JUTEAU, J. P. EBERHART, J. C. TOURAY and P. BAILLIF, *Geochim. Cosmochim. Acta* **47** (1983) 377.
7. J. L. CROVISIER, J. HONNOREZ and J. P. EBERHART, *ibid.* 51 (1987) 2977.
8. E. VERNAZ and J. L. DUSSOSSOY, *Applied Geochem.* (Suppl. 1) (1992) 13.
9. S. RICOL, Thesis, Univ. P. and M. Curie, Paris, 1995.
10. B. C. BUNKER, D. R. TALLANT, T. J. HEADLEY, G. L., TURNER and R. J. KIRKPATRICK, *Phys. Chem. Glasses*, **29** (1988) 106.
11. W. H. CASEY and B. C. BUNKER, *Rev. Mineralogy* **23** (1990) 397.
12. P. AAGAARD, H. C. HELGESON, *Am. J. Sci.* **282** (1982) 237.
13. B. GRAMBOW, in Scientific basis for nuclear waste MRS Symposium Proc. Vol. 44 (Mater. Res. Soc., 1985) p. 15.
14. E. Y. VERNAZ and N. JACQUET-FRANCILLON, *Verre* **3** (1997) 14.
15. P. BAILLIF, B. CHOUIKHI, L. BARBANSON and J. C. TOURAY, *J. Mater. Sci.* **30** (1995) 5691.
16. B. CHOUIKHI, Thesis, Univ. d'Orléans, Orléans, 1995.
17. H. SCHOLZE and R. CONRADT, *Ann. Occup. Hyg.* **31** (1987) 683.
18. R. M. POTTER and S. M. MATTSON, *Glastech. Ber.* **64** (1991) 16.
19. B. C. BUNKER, G. W. ARNOLD and J. A. WILDER, *J. Non-Crist. Solids* **64** (1984) 291.
20. R. K. ILER, in "The Chemistry of Silica" (John Wiley and sons, New York, 1979).

Received 30 October 1998
and accepted 9 April 1999